

SIF2004 Structural Integrity and Fracture. <http://eprint.uq.edu.au/archive/00000836>

## Probabilistic Aspects Of Brittle Fracture In Pressure-Vessel Steels

J F Knott

The University of Birmingham, U.K.

**ABSTRACT:** This paper addresses issues relating to the treatment of distributions of tensile strength, local cleavage fracture stress, and fracture toughness in pressure-vessel steels and weld deposits. Attention is drawn to the differences in behaviour between steels which have “quasi-homogeneous” microstructures and those which exhibit spatial heterogeneity. The differences are of greatest significance when statistical analysis is applied to distributions to derive “lower-bound” values. The findings from model systems are used to re-assess an earlier analysis of Weibull fracture stress and to comment on the use of a Master Curve methodology in the analysis of the “Euro” fracture toughness data-set.

### 1 INTRODUCTION

The scatter associated with the measurement of a mechanical property, such as flow strength or toughness, is of importance because it forms part of the overall probabilistic failure assessment of a structure. Fracture toughness distributions may be fitted by a variety of statistical formulations, but, if these are not related to a physically-based model, there is concern that the tail of a distribution (to which the overall failure probability is highly sensitive) does not have the appropriate form. The modelling behind the “local approach” or Weibull methodology [Beremin 1983] is based on a “test volume” concept. The linear dimension of a “process zone” is proportional to  $K^2$  and so the process zone area is proportional to  $K^4$ . This is also a part of the Curry/Knott [1979] treatment of cleavage fracture. The test volume is then taken to be proportional to the length of the crack front (in test-pieces, the test-piece thickness,  $B$ ) multiplied by  $K^4$ . This enables values of Weibull parameters to be compared for different test volumes. For low probability events, a lower bound needs to be set. This may be at some level of probability appropriate to a particular safety case (e.g.  $10^{-4} = 0.01\%$ ) or expressed as a number of standard deviations (s.d.) below the mean (3.09 s.d. = 0.1%). Both an assumed Gaussian distribution or a two-parameter Weibull (with a cut-off value of zero) require that this lower bound be set independently. A three-parameter Weibull includes a “cut-off” value in its formulation, but a robust methodology needs to be established to establish its value. [Neville and Knott 1986]. It may be of significance to note that the value chosen for the “cut-off” affects the value of Weibull modulus, so that the usual interpretation of a Weibull modulus as representing the degree of scatter in a data-set becomes somewhat ambiguous. The “Master Curve” method [ASTM 2002] includes an independent cut-off of  $20 \text{ MPa m}^{0.5}$ . This value is taken as constant for a range of pressure-vessel steels (once the reference temperature,  $T_0$ , corresponding to a median fracture toughness of  $100 \text{ MPa m}^{0.5}$  has been determined) and is also constant throughout the whole transition range for which the Master Curve applies (a range of over 150K). Results given later in this paper suggest however, that, for a wider range of steels, this single value underestimates the lower bound for some steels/heat-treatments and overestimates it for others. It might also be expected that the “cut-off” value would vary, if weakly, with temperature, reflecting the decrease of yield strength with increase in temperature. In an application of Master Curve methodology to the “Euro” data-set, Wallin [2002] used both the standard value, and also “fitted” values for individual data sets. Interestingly, some of these “fitted” values were *negative*. As will be seen below, this is a strong indicator of heterogeneity in material, but the raw findings highlight the dangers inherent in the simple fitting of a standard

statistical form to a distribution, without paying due recognition to microstructures and micro-mechanisms of fracture.

Even for wrought products, common structural steels are unlikely to possess spatially uniform properties, because chemical segregation in the original casting may persist throughout the working processes. There may be a spatial distribution of non-metallic *inclusions*, which affect the critical value of  $J_i$  the J-Integral, or  $\delta_i$ , the crack-tip opening displacement (CTOD), at the initiation of ductile fracture; a spatial distribution of *major alloying elements*, which, through their effects on *hardenability*, influence transformations and the toughnesses of transformed microstructures; and a spatial distribution of *trace impurity elements*, which can induce inter-granular embrittlement. Similar factors, on a coarser scale, affect multi-pass weldments [Todinov *et al.* 2000]. It may be noted, in terms of flow properties, that the 0.2% proof strength is likely to show more variability in spatially heterogeneous material than is the UTS, because the proof strength reflects the resistance to the production of a macroscopic plastic strain of just 0.2%: this could well be accomplished by plastic deformation in only the softest microstructure present. The UTS is a property reflecting the total behaviour of all microstructures present, deforming as a continuum. The point has been clearly illustrated for an as-deposited C-Mn weld metal [Tweed and Knott, 1987]. Here, it was shown that the softer grain-boundary ferrite strained by up to ~7% until it had hardened to the same level as that of the acicular ferrite. From then on, both microstructures deformed equally.

Recent work has attempted to distinguish between the fracture toughness properties of *quasi-homogeneous* and *heterogeneous* materials. No engineering material is truly homogeneous, but, if a steel contains a high volume fraction of relatively small carbides, distributed in a smooth “well-behaved” fashion, a large number of potential crack nuclei will be sampled in the process-zone. Whether the “critical” size is taken as the 95th or 98th percentile, the size of the particle,  $c_o$ , in the “well-behaved” distribution will not vary by any large amount from sample to sample and the critical fracture stress, which depends on  $c_o^{-0.5}$  will be, to all intents and purposes, single-valued. This implies that values of the local fracture stress,  $\sigma_F$ , in notched bars fractured at low temperatures should be single-valued (within the limits of random experimental errors) and it further follows that the size of the process zone and the value of  $K$  at fracture in fracture toughness tests should be the same for whichever sample in a batch is tested. The following sections discuss the extent to which these concepts are validated and how working definitions of “quasi-homogeneous” and “heterogeneous” behaviour may be established.

## 2 VARIABILITY IN ULTIMATE TENSILE STRENGTH

The aim of this section is to show how use of a basic model can be used to predict the form of a statistical distribution, which can then be compared with experimental values. The model for UTS uses Considère’s criterion, which balances the rate of strain-hardening against the loss of cross-sectional area as a specimen undergoes plastic deformation (as a uniform continuum). If the material’s true stress ( $\sigma_t$ ) – true strain ( $\epsilon_t$ ) curve is represented by the form,  $\sigma_t = K\epsilon_t^n$ , the criterion for necking is given by  $\epsilon_t = n$ , giving the true stress at the UTS as  $Kn^n$  and the UTS, which equates to the nominal stress ( $\sigma_{nom}$ ) =  $\sigma_t (A/A_0)$ , where  $A$  is the area at the UTS and  $A_0$  is the original area, as:

$$UTS = \sigma_{nom} = Kn^n / (\exp n) \quad (1)$$

Equation (1) predicts that the value of the UTS is determined by the parameters  $K$  and  $n$  in the relationship between true stress and true strain. These may be taken as constant for uniform, homogeneous material of constant grain size and heat-treated/cold-worked condition. The *prediction of the model* is that the UTS is a *single-valued* parameter.

There is value in presenting distributions in graphical form. The *probability density function*, pdf, is the histogram of the number of occurrences of a particular value as ordinate, plotted *versus* the range of values on the abscissa. For a single-valued parameter, the pdf is a delta (spike) function, located, in this case, at the value of the UTS. The *cumulative distribution function*, CDF, is the integral of the pdf, representing the number of occurrences of the range of values up to a point of interest: it is usually scaled as a fraction or percentage of the total number of values. For a single-valued parameter, the CDF is a step function, having a value of zero up to the UTS, and unity (or 100%) above the UTS. In any set of experimental results, there are experimental errors. Here, these are assumed to be small and randomly distributed about the mean. The *central limit theorem* [Sokolnikov and Redheffer 1966] shows that *random errors* are distributed in a *normal* manner about the mean. For a single-valued parameter, the pdf is then a Gaussian distribution (with a standard deviation s.d. reflecting the degree of variation in random variables) and the CDF is the error function, *erf*, which is the area under the Gaussian, but scaled by a factor of  $2/\pi^{0.5}$  to provide a value of unity for the total range. For a second steel/heat-treatment, having a different UTS, the effect is *to shift the value of the mean*, but *not* to alter the s.d. because the random experimental errors have not changed. (Noting that, in the absence of any such errors, equation (1) predicts both UTS values to be delta functions). The *ratios* of s.d. to mean will, however, be different, because the means have shifted. It is useful to represent the CDF on *normal probability paper*, which has its ordinate scaled about 50% (or 0.5) so that the erf plots as a straight line:  $\pm$ one s.d. corresponds to frequencies of 16% and 84%. Median ranking is employed, with the median rank of order  $n$ ,  $F_n$ , in a set of total number  $N$ , derived from the close approximation [Bompas-Smith 1973]:

$$F_n = (n - 0.3) / (N + 0.4) \quad (2)$$

Fig. 1 shows the CDFs for UTS values in PWR pressure-vessel steels [Marshall 1982]. Attention is drawn first to the “French” data (69 samples) for A533B Class1, which conform to linear behaviour, with a mean of 617 MPa and s.d.  $\pm 19$  MPa, approx. 3% of the mean. Similar values (614  $\pm$  15 MPa) were obtained by the Japanese for A533B Class1. Although the s.d. values may reflect some genuine material variability from sample to sample, arguably they simply reflect random experimental test variables (variations in load measurement, measurement of cross-sectional area, precision of identifying the position of the load maximum etc.). If so, they are predicted, by the Central Limit Theorem, to be distributed about the mean in a Gaussian manner. For the purposes of this paper, this is what is assumed, and with this assumption, it becomes clear that the *basic prediction* of the UTS *model* is *supported*: in homogeneous material, the UTS is a single-valued function. A second set of “French” data (61 samples), for A508 Class 3, have a similar mean, 612 MPa, but a somewhat larger s.d.  $\pm 29$  MPa, 4.8% of the mean. Since the care taken in tensile testing may be assumed to be of similar quality for both sets of French material, the increase in s.d. is now more likely to reflect a degree of material variability from sample to sample. The level of variability is, however, unlikely to give rise to concern in general structural integrity assessments. A -2 s.d. lower bound would be 554 MPa, derived from the mean of 612 MPa (contrasted with 579 MPa, 617 MPa). Since safety factors of 2 are applied to the yield strength for the initial design of PWR steels, this decrease (and the difference between the

two batches of steel) is insignificant. Similar changes to the flow strength, affecting the position of an assessment point on the  $L_r$  abscissa on the R6 Failure Analysis Diagram, are, again, unlikely to cause problems, except in extreme circumstances, where the assessment point ( $K_r, L_r$ ) is already close to the near-vertical part of the failure locus. Results for American PWR steels gave s.d. values of about 30 MPa (5% of the means).

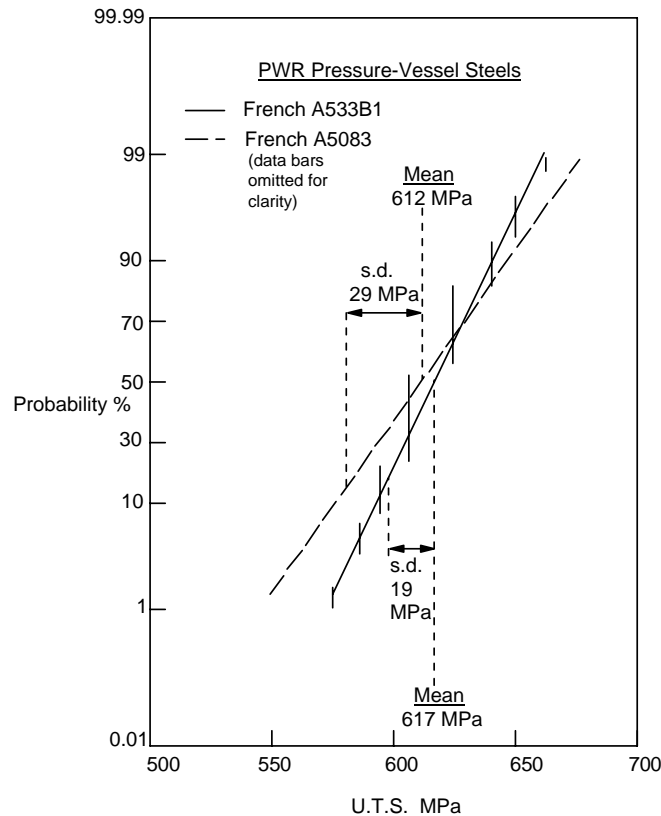


Figure 1 Cumulative distribution functions for UTS values in PWR steels  
 Data from Marshall (1982)

In lower strength steels, there are significant changes, particularly of yield strength, but also of flow strength, with grain size. A large block of material, cooled from high temperature, may contain a range of grain sizes throughout its cross-section, as a result of the different cooling-rates experienced by near-surface and central regions. This is recognised in specifications for steel plate, where thicker plates do not have as high a guaranteed lower-bound yield strength as that stipulated for the same composition in thinner section. Tensile test samples from surface layers of thick sections will exhibit a high mean yield strength, representative of homogeneous fine-grained material with a low s.d. (reflecting random experimental errors). Samples from the centre will exhibit a lower mean, representative of homogeneous coarse-grained material, again associated with a low s.d. A range of samples from all positions throughout the section will have an intermediate mean value, but with a higher s.d. attributable to the fact that not all samples belong to the same “metallurgical” population.

### 3 VARIABILITY IN LOCAL FRACTURE STRESS IN NOTCHED BARS

The sequence of events leading to cleavage fracture ahead of a notch in steel at low test temperatures is that plastic deformation nucleates a micro-crack in a brittle second-phase particle, which then propagates under the influence of a critical tensile stress,  $\sigma_F$ . It is found experimentally that the value of  $\sigma_F$  is independent of temperature over a range of low temperatures [Knott 2000]. The brittle particle may be a carbide, an inclusion (such as an oxide or silicate), or titanium carbo-nitride. The values of  $\sigma_F$  are determined by measuring the fracture load in a notched bar, and using an elastic/plastic finite element stress analysis to determine, either the *maximum* value of local tensile stress ahead of the notch [Griffiths and Owen 1971] or a *characteristic* stress, which represents an averaged stress across the notched cross-section [Beremin 1983]. The treatment of scatter in the latter case is to fit values of the characteristic stress to a Weibull distribution. Drawing on the results of a number of studies [Curry and Knott 1979, Tweed and Knott 1987, Knott 2000] it is possible to develop a micro-mechanical *model* for cleavage fracture as the Griffith-like propagation of a disc-shaped micro-crack nucleus from a brittle particle:

$$\sigma_F = \{\pi E \gamma_p / 2(1 - \nu^2) c_0\}^{0.5} \quad (3)$$

where  $c_0$  is the radius of the micro-crack,  $E$  is Young's modulus,  $\nu$  is Poisson's Ratio and  $\gamma_p$  is the local work of fracture, found experimentally to be of order 9-14 J m<sup>-2</sup>. [Knott 1994]. The scatter in  $\sigma_F$  values, from *test-piece to test-piece*, is then related to the *probability* of finding a *given size of particle* in the *high stress region* ahead of a notch, at a given applied load. For the failure loads and notched bar geometry commonly used, the region ahead of the notch in which the local stress rises from 0.95  $\sigma_{max}$  to  $\sigma_{max}$  and then falls to 0.95  $\sigma_{max}$  is of order one root radius (0.25mm). The lateral extent is of similar dimension. Although the size distribution of brittle particles is not normal: there being many small, and fewer large, particles; it is argued that, if a "typically large" (say, 95th percentile) particle is *consistently* sampled, from test-piece to test-piece, closely similar values of  $\sigma_F$  will be produced. The fracture stress varies as the inverse square root of particle size.

The predictions of the model may be tested, using results [Wu and Knott 2004] for a reproduction weld metal, both in an as-received condition and after an embrittling treatment, which coarsened the grain size, and caused the material to become susceptible to inter-granular embrittlement, by promoting the segregation of impurity elements to grain boundaries. The material was further subjected to 8% cold prestrain. The brittle particles acting as cleavage initiation sites were non-metallic inclusions, typically some 2  $\mu$ m in size, representing the 95th percentile. For a similar weld metal, 309 inclusions (following a log-normal distribution) were found [Widgery and Knott 1978] in an area of 14450  $\mu$ m<sup>2</sup>, i.e. approx. 0.12 mm x 0.12 mm; of order 1200 are then expected in the 0.25 x 0.25 mm<sup>2</sup> high stress region ahead of a notch – hence 60 of the 95th percentile size. A "weakest link" argument is not strictly sustainable, but the figures show that, if a series of micro-fractures is triggered-off in an "avalanche" once a crack starts to spread from the most susceptible particle, so many particles are present in the high stress region that all test-pieces are expected to behave in near-identical manner. The distribution of  $\sigma_F$  is *predicted* to be *single-valued*. With random errors, the CDF, on *normal* probability paper, is predicted to be linear, with small s.d., reflecting the random experimental errors.

Fig. 2 shows the experimental CDF distributions for  $\sigma_F$  for the two conditions. The distributions are seen to be linear, with different means: 1555 MPa and 1400 MPa, but with similar values of s.d. 35 MPa: 2.2% and 2.5% of the mean respectively. The prediction is therefore confirmed: the CDFs are straight lines with s.d. values which are small, noting that they are obtained from a combination of load and finite-element stress analysis. Wu and Knott estimated experimental and numerical errors to be of order  $\pm 80$  MPa ( $\pm 2.3$  s.d.) and all data points for either condition were found to lie within these bounds. (Note that the s.d. for the UTS distribution in Fig.1 for material assumed to be homogeneous is  $\sim 3\%$  of the mean). The embrittlement procedure has decreased the local fracture stress of the weld metal, effectively by lowering the work-of-fracture,  $\gamma_p$ , in Eqn (3). It has not, however, altered the distribution of crack-initiating particles in any given test-piece or the random experimental errors which have been identified as the primary cause of scatter in the results. The absolute values of s.d. are identical, although they vary as a proportion of the mean. The results obtained here for “reproduction” (carefully fabricated) weld metal are more typical of those for wrought products than of those for welds in general. These may contain a much wider size-range of inclusions: both as the expected de-oxidation products (up to  $\sim 4$   $\mu\text{m}$  in size) and “exogenous” inclusions, which may enter the weld pool from an unexpected source e.g. from the binder for the coating on a welding rod. An isolated inclusion of this sort of size 10  $\mu\text{m}$  has been observed [Tweed and Knott 1987]. This would produce a clearly observable “outlier” to any predicted CDF, as an unexpectedly low value of  $\sigma_F$  or, perhaps, as a “pop-in” at low applied load. Such an anomalous point provides an incentive for further investigation, identification of its cause and subsequent remedial action.

The data in Fig. 2 have been drawn to 1% and 99% limits (approx.  $\pm 2.3$  s.d.(80 MPa) - the estimated maximum experimental error) and show a small overlap between the lowest “as-received” condition and the highest “degraded” condition. This is a slight extrapolation beyond the range of the experimental results, for which the highest “degraded” value was 1462 MPa (at the 97.5% level) and the lowest “as-received” value was 1482 MPa (at the 97% level). Consider now the analysis if it were *not initially known* which test-pieces were “as-received” and which were “degraded”, such that the whole set was treated as a single population. The resultant re-plotting of data is shown in Fig. 3. There are now two branches, reflecting the original distributions at the lowest and highest values, joined by a central portion, reflecting the “uneasy marriage” of the two separate distributions (forced by the assumed lack of knowledge). The separation is more clearly seen for the normal CDF than for a Weibull representation, and provides a “template” for the diagnosis and analysis of distributions.

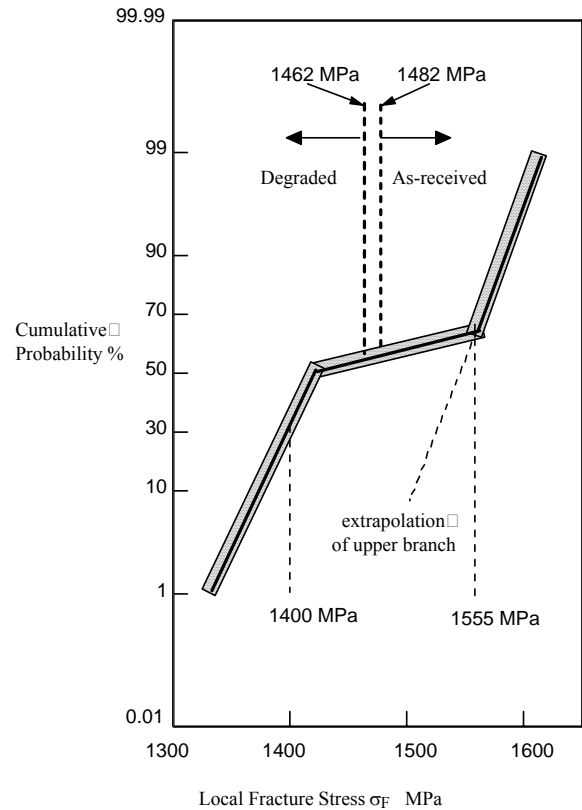
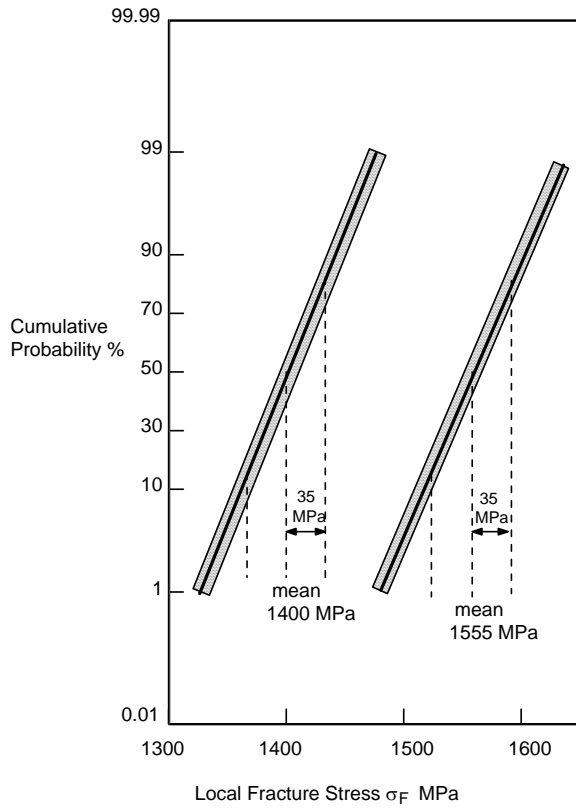


Figure 2 CDF distributions of local cleavage fracture stress for as-received and “degraded” weld metal – data from Wu and Knott (2004)

Figure 3 The data from Fig. 2 re-plotted as if for a single distribution

*The presence of sharp changes in slope (not predicted by the physical model), demands thorough investigation.* Given the results in Fig.3, it would be necessary to undertake fractographic and metallographic examination, ideally on all specimens, but particularly on those whose fracture stresses spanned the central region. It would then be found that those which had failed at stresses at and above 1482 MPa would reveal trans-granular failure and relatively fine grain size; those failing at and below 1462 MPa would reveal inter-granular fractures and large grain sizes. These observations then provide justification for re-analysing the two sets as different populations, with the results shown in Fig. 2. These data are clear-cut, with overlap occurring only at the 1%/99% level. More overlap could confuse the details, but, once a change (or changes) in slope has revealed the presence of two (or more) populations, the degree of confidence in their independence can be assessed by conventional techniques such as Student's t-Test. The *detection of slope changes* (based on the visual “template” in Fig.3), *not predicted by the underlying model*, is, however, a critically important first step in the statistical analysis. Slope changes may be seen but are less easy to interpret in the Weibull presentation. The

“ln.ln.vs. ln” scales tend to provide too close a grouping of points and the predictive model is less clear. To clarify the “change in slope”, consider equal numbers of samples of two steels with different “ideal” UTS values. From equation (1), each pdf is a delta function, each CDF a step function. The CDF for the combined set is a double-step function: two vertical “risers” below and above 50% probability and no values on the horizontal “tread”. The incorporation of random errors transforms the “risers” to two steeply sloping lines and the “tread” to a shallow slope: see Fig. 3.

The Wu and Knott paper [2004] used the approach to re-assess some of the Beremin [1983] analyses of fracture stress results. In the original paper, results for A508 steel were analysed by means of a two-parameter Weibull. The results for steel Heat A were stated to give a Weibull modulus  $m=22$ , although subsequent regression analysis of the published data gives  $m=13.3$ . This is still a high value and the distribution could therefore be equally well plotted as a normal CDF, since the Weibull and Normal distributions are virtually identical for  $m>4$  [Bompas-Smith 1973]. This was done by Wu and Knott to derive mean and s.d. values of 2493 MPa and 221 MPa, 9% of the mean. It is of interest to compare these results with the values for the weld metals treated as a single, or two separate, distributions (Figs. 3 and 2). The distribution in Fig.3 as a single population of the results from the two different conditions gives a value of  $m = 19$ , corresponding to a mean of 1477 MPa and a “standard deviation” of 89 MPa (6% of the mean). The value of “standard deviation” for the Beremin results, 221 MPa (9% of the mean), is significantly larger than this figure (which is, of course, already for the “combined” distribution). Since there is no reason to suppose that random experimental errors in the Beremin work were any greater than for the present experiments (approx. 2.4% of the mean for the separate distributions), it may be conjectured that the Beremin results reflect spatial heterogeneity in the material. Bowen *et al* [1986] have measured  $\sigma_F$  values for a number of different simulated microstructures in A533B (a steel very similar to A508), obtaining values in the range of 2000-3500 MPa, which spans those for Beremin’s Heat A. Generally, this range splits into two bands. The lower values correspond to coarse ferrite/carbide distributions (pearlite, coarse upper bainites); the higher values to fine distributions (tempered martensites, lower bainites). Wu and Knott carried out a sensitivity study on 10 or more data points in the “lower branch” of the Beremin distribution to try to detect sub-sets. Points ranked 4 to 13 gave a mean of 2319 MPa with a standard deviation of 56 MPa (2.4% of the mean) and a total error range of approximately  $\pm 85$  MPa. The Weibull modulus for these 10 points was 46, similar to those for the separate distributions in Fig.2. It was inferred that this set of points *could* represent an independent subset. If generic to French A508 steel, the presence of spatial heterogeneity is consistent with the finding that the s.d. for the A508 UTS distribution was higher than that for the UTS distribution (Fig.1).

#### 4 THE FRACTURE TOUGHNESS OF “QUASI-HOMOGENEOUS” STEEL

The model adopted to treat the fracture toughness of steel follows the RKR model [Ritchie, Knott and Rice 1973] for cleavage fracture in mild steel. This identified a *critical distance*,  $X$ , needed to reconcile the dimensions of local fracture stress,  $\sigma_F$  (stress) and fracture toughness,  $K_{Ic}$  (stress x length<sup>0.5</sup>). In a study of cleavage fracture in spheroidised microstructures [Curry and Knott 1979],  $X$  was defined in terms of a *statistically-averaged distance*, with the *microstructure* characterised in terms of the histogram of number density (per unit volume, or per unit area in 2-D) of carbides as a function of carbide radius,  $c_o$ . The local value of  $\sigma_F$  (in notched bars) was calculated for each radius. Reference was then made to the tensile stress distribution in the process zone ahead of a crack loaded to a given stress-intensity factor,  $K$ , and the stress “available” at a given position  $r$ ,  $\theta$  was compared with the probability that, at this position, there would be a carbide of radius sufficiently large for a newly-



initiated (disc-shaped) microcrack to propagate at this level of local stress. If this were not the case for any  $r, \theta$  values at a given applied  $K$ , the value of  $K$  was increased until the condition was met (at  $K = K_{IC}$ ). A similar approach has been adopted by Lin, Evans and Ritchie [1986, 1986a]. Any variation in  $K_{IC}$  is related to the distribution of carbide sizes. For the spheroidised steels (uniformly austenitised, quenched and tempered) the distribution is smooth and continuous and there is a high probability that a “typically coarse” (95th or 98th percentile) carbide will be found *consistently* in an equivalent  $\sigma(r, \theta)$  position for a given applied  $K$  value, so that systematic variability from test-piece to test-piece should be small. This conclusion is supported by measurement [Neville and Knott 1986] of a number of fracture toughness values at  $-115^\circ\text{C}$  in samples of En8 steel, quenched from  $810^\circ\text{C}$  and tempered at  $220^\circ\text{C}$  for 1 hour. A normal distribution was obtained, with a mean of  $32.4 \text{ MPa m}^{0.5}$  and s.d. of  $1.03 \text{ MPa m}^{0.5}$  i.e. 3.2% of the mean. (All results fell within 6% of the mean). Random experimental errors were estimated as only  $\pm 2\%$  and it was shown that, even within the narrow  $K_{IC}$  distribution, there was sufficient variability in the hardness of different samples (592-609 VDH) to produce a small systematic variation in the  $K_{IC}$  values. Fracture toughness distributions for other fine-scale steel microstructures are discussed below.

In the Beremin [1983] “local approach”, the (averaged) local fracture stresses are assigned to a Weibull distribution. Stress distributions around a crack tip at a given  $K$ -level are analysed and the probability that the stress at a given  $r, \theta$  position in the plastic zone exceeds the “Weibull stress” is assessed. If the *maximum local stress* in a cylindrically notched test-piece were used, this would equate to the input fed into the original RKR model. In more recent work, particularly on weld metals, it is possible to determine the value of stress at the initiation site in the notched bar or the pre-cracked fracture toughness specimen. In the “Local Approach” the *concept* of a “critical distance” is still necessary (although it is defined differently) and is, in one example,  $\sim 0.25\text{mm}$  (in RKR, using  $\sigma_{\max}$ ,  $X = 0.12\text{mm}$ ). The Beremin use of the “Weibull stress” does not relate it to any micro-structural feature, such as the carbide distribution, and the Wu and Knott [2004] re-analysis of the Beremin results, discussed above, allows the possibility that this lack of correlation could lead to inappropriate analysis, e.g. using an average Weibull stress derived from a distribution containing results for both fine and coarse microstructures to treat a crack tip located predominantly in either a fine, or a coarse, microstructure.

The tensile stress model relates to *transgranular cleavage* or *intergranular* fracture, in which the critical event is the propagation of a brittle micro-crack. In low strength steel, the *ductile fracture* process is dominated by the *internal necking* between, and *coalescence* of, voids initiated on non-metallic inclusions. In a microstructure containing ferrite grains, grain-boundary carbides and non-metallic inclusions, there is a clear separation between the value of fracture toughness for brittle fracture and that for ductile fracture. In high-strength steels, the transition is less distinct. High strength is produced by microstructural refinement and a high volume-fraction of closely-spaced particles, combined with a high density of transformation dislocations. Proof strengths of over 1500 MPa can be generated in low-alloy steels, quenched and tempered in the range  $300\text{-}450^\circ\text{C}$ . The cleavage fracture process, below the transition temperature, is similar to that for En8 steel [Neville and Knott 1986].

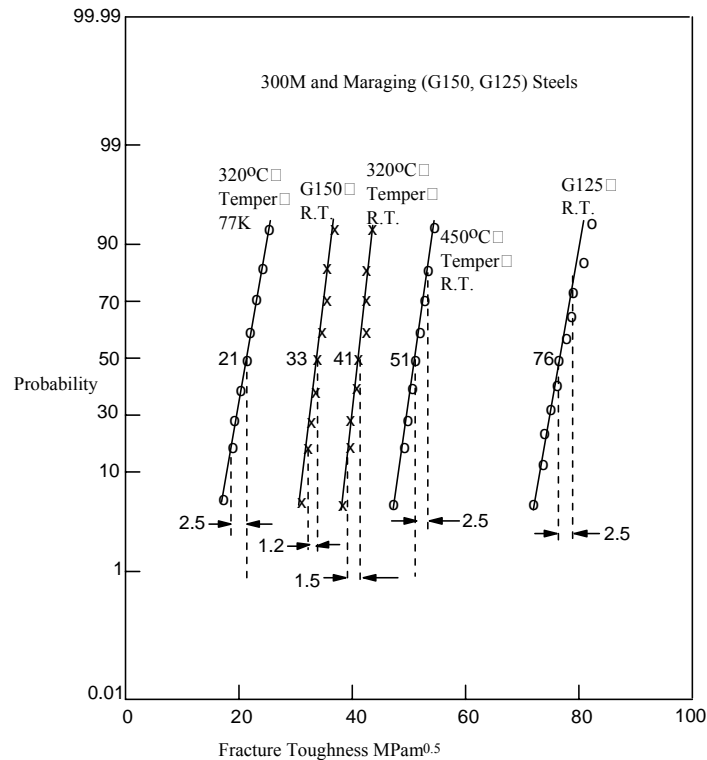


Figure 4 CDF plots for the distributions of fracture toughness in 300M and maraging steels – data courtesy Dr J E King and Dr B Wiltshire

Above the transition temperature, ductile fracture initiates by the formation of voids on non-metallic inclusions, but linkage does not occur by the “internal necking” process. Instead, the accumulating plastic strain between expanding voids, comprising dislocations looped around the carbide hardening particles, causes carbide/matrix interfaces to decohere, leading to a “fast-shear” linkage. The overall strain/toughness associated with this process can be quite low. In the “cleanest” (lowest inclusion content) high-strength steels, the ductile fracture is dominated by fast shear, and since this operates on the scale of the tempered carbides, the material is expected to behave in a “quasi-homogeneous” manner. It is predicted that once a high-strength steel is sufficiently clean (in terms of inclusions), no improvement in fracture toughness will be obtained by a further decrease in inclusion content (increase in spacing) because the fracture process is dominated by carbide/matrix de-cohesion [Smith, Cook and Rau 1977, Slatcher and Knott 1982]. The effects of these features on fracture toughness distributions are illustrated in Figs. 4 and 5 which show CDFs, plotted on normal probability scales, for 300M and G125, G150 maraging steels, used in aerospace applications, and for a QT steel used in gun barrels. In Fig. 4, the data for 300M [King and Knott 1980] indicate “quasi-homogeneous” behaviour, at both  $-196^{\circ}\text{C}$  (cleavage fracture) and room-temperature (cleavage and micro-voids). The values of s.d. are  $\pm 2.5$ ,  $\pm 1.5$  and  $\pm 2.5$   $\text{MPa m}^{0.5}$ . The values for G150 and G125 [Wiltshire and Knott 1980] are  $\pm 1.2$  and  $\pm 2.5$   $\text{MPa m}^{0.5}$ . For 300M, the room-temperature fracture toughness is greater for the  $450^{\circ}\text{C}$  temper than for the  $320^{\circ}\text{C}$  temper. This is due to “ $350^{\circ}\text{C}$  embrittlement”, arising from a balance between inter-lath cementite development and matrix softening. The  $320^{\circ}\text{C}$  temper has a proof strength of 1900 MPa, compared with 1500 MPa for the  $450^{\circ}\text{C}$  temper.

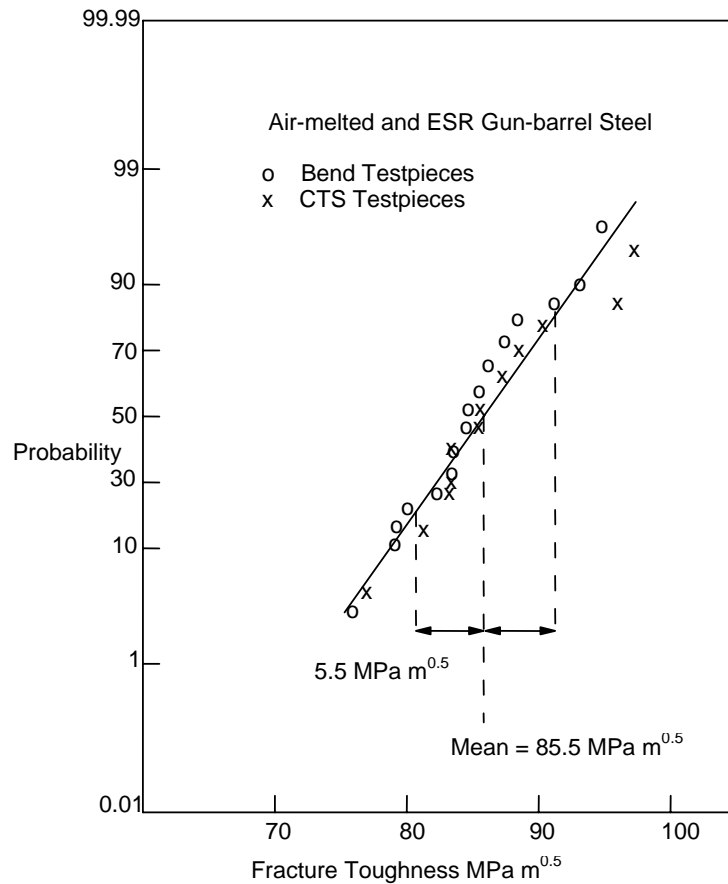


Figure 5 Cumulative distributions of fracture toughness for a gun-barrel steel  
Data courtesy Dr S Slatcher

Fig. 5 shows fracture toughness results [Slatcher and Knott 1982] for a gun-barrel steel (0.34C 3.2Ni 0.8-1.15Cr 0.7Mo), initially ignoring small variations in the material's chemistry, processing route and heat-treatment. The s.d. is  $\pm 5.5 \text{ MPa m}^{0.5}$ . The values obtained from SEN Bend and CTS test-pieces were agreeably similar. Some test-pieces were cut from air-melted (AM) stock (with 1.15Cr); others, from electro-slag-refined (ESR) stock (with 0.8Cr). The CDFs for the two conditions were found effectively to superimpose. This is as predicted, because both AM and ESR material had low inclusion contents and the fast shear process is dominated by de-cohesion of the carbide/matrix interfaces. An effect of tempering temperature could be deduced: as for 300M, the 300-350°C tempers were less tough than the 400-450°C tempers (although the yield stress had decreased only slightly, from  $\sim 1400 \text{ MPa}$  to  $\sim 1300 \text{ MPa}$ ). The s.d. values did not drop to the  $\pm 2-3 \text{ MPa m}^{0.5}$  level, suggesting that further variables, e.g. the spatial location of a test-piece in a forging would be needed to be explored to produce more convincing "quasi-homogeneous" behaviour. In general more variability is to be expected here than in high-quality aerospace alloys and, for service application, the s.d. of  $\pm 5 \text{ MPa m}^{0.5}$  may be acceptable. A review of other data-sets for steels of this type [May 1965] suggests that a pragmatic value for the s.d. of material to be defined as "quasi-homogeneous" is  $\pm 5-6 \text{ MPa m}^{0.5}$ .

## 5 THE FRACTURE TOUGHNESS OF “HETEROGENEOUS” STEEL

The behaviour of quasi-homogeneous material contrasts sharply with that for spatially heterogeneous material [Zhang and Knott 1999, 2000]. Cleavage fracture-toughness values were measured at  $-80^{\circ}\text{C}$  for A533B pressure-vessel steel, heat-treated to generate three microstructures: 100% (autotempered) martensite,  $\alpha'$ ; 100% (coarse) upper bainite,  $\beta$ ; 30%  $\beta$ , 70%  $\alpha'$ ; all with a prior austenite grain size of  $250\mu\text{m}$ . Fig. 6 shows that the CDFs for 100%  $\alpha'$  and 100%  $\beta$  plot as “quasi-homogeneous” functions, with s.d. values less than  $6\text{MPa m}^{0.5}$ . Interest lies in the behaviour of the 30%  $\beta$ , 70%  $\alpha'$  mixture. Due to carbon and alloy segregation in the melt and/or during processing, the hardenability of the material is not spatially uniform and the microstructure consists of a “patchy” mixture of “brittle” bainite ( $\beta$ ) and “tough” martensite ( $\alpha'$ ). There is also a systematic spatial variation of the proportion of bainite (from 15% to 45%) over a “wavelength” of some  $250\text{-}500\mu\text{m}$ . In a set of fracture-toughness tests, the critical region ahead of the crack tip may, in some specimens, be located in a region with a high amount of “brittle” bainite and, in others, a low amount. It is, therefore, expected that the CDF for the mixed microstructure lies between “tramlines”, bounded by the CDF for  $\beta$  and the CDF for  $\alpha'$ . Fig.6 shows that this is what is observed. A “best-fit” straight line drawn through the data-points exhibits a s.d. of  $20\text{MPa m}^{1/2}$ , or 33% of the mean (over three times that for  $\alpha'$  or  $\beta$ ). A single straight line is, of course, not appropriate, and, although there are rather few data points, there are suggestions, following the “template” of Fig. 3 that the distribution is (at least) bi-modal. The material is not “quasi-homogeneous” and the physical reasons for this are clear. Fitting the data empirically to (two-parameter) Weibull distributions gives  $m = 14.5$  for 100%  $\beta$  and  $m = 3.2$  for 30%  $\beta$ , 70%  $\alpha'$ .

This metallurgical system was designed to demonstrate a point of general applicability to “heterogeneous” microstructures. These include not only micro/meso-scale variations in heat-treated forging steels, but also meso/macro-scale variations in multi-pass welds and nano/micro/meso-scale variations in the segregation of “embrittling” species (such as P, Sn, Sb) to grain boundaries in quenched-and-tempered steels [Islam, Bowen and Knott 2001]. The spatial extent of a “coarse” or a “fine” region in a multi-pass weld is a few mm. The root radius of a Charpy notch is 0.25 mm and the extent of uniform high stress is similar. It is found that wide scatter in toughness is obtained for weld deposits, not only in sharply-cracked testpieces but also in Charpy tests [Newmann, Benois and Hibbert 1968, Todinov *et al.* 2000].

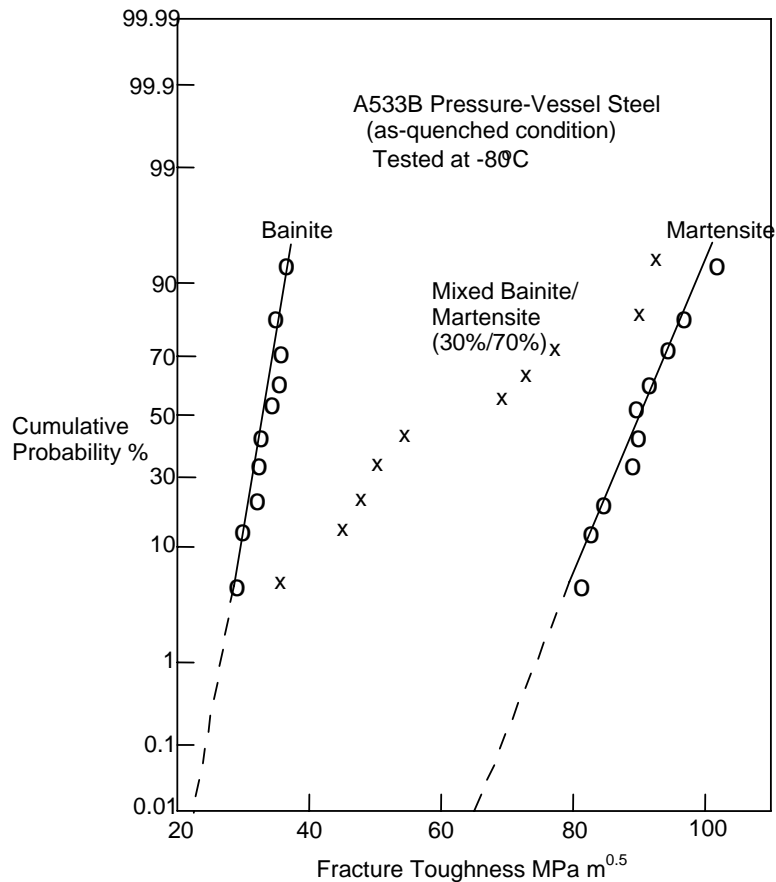


Figure 6 CDF plots for the fracture toughness at  $-80^{\circ}\text{C}$  of A533B, austenitised at  $1250^{\circ}\text{C}$ , grain size  $\sim 200\ \mu\text{m}$  – after Zhang and Knott (2000)

A final point relates to the use of statistical analysis to derive “lower-bound” values for fracture toughness, typically at a level of  $10^{-4}$  (0.01%). Such values may be required for the establishment of an acceptably low probability of failure for critical engineering plant. For quasi-homogeneous material, it is reasonable to extrapolate the CDF to the required level, recognising that, if an out-lier is found, its cause must be investigated. For 300M (Fig. 4), the lower-bounds, at the 0.01% level, are 12, 36 and  $39.5\ \text{MPa m}^{0.5}$ , whereas, for the 100% martensite and 100% bainite CDF distributions in Fig. 6 they are  $65\ \text{MPa m}^{0.5}$  and  $22\ \text{MPa m}^{0.5}$ . For the mixed microstructure, extrapolation to 0.01% probability gives a value which is not just much *lower* than the lower-bound for *the more brittle constituent*, but is *negative!* This is equivalent to the negative values obtained by Wallin’s “fitting” of cut-off values to the Euro data base, using Master Curve methodology. The physical reasons for the negative value are clear when Fig. 6 is examined, because the limiting “tramlines” are clear, but consider a situation for which the *only data-set available* were that for 30% $\beta$  70% $\alpha'$  material. In the absence of a model, these data would be fitted empirically to a Weibull distribution, as has been done by Wallin, and the negative value would be obtained. The “common sense” lower bound *can* be established by setting the value for the mixed microstructure equal to that for the more brittle bainite phase, but the clarity of Figs. 4-6 is obscured by the rather convoluted Weibull presentation. The present Master Curve recommendation of

a cut-off value of  $20 \text{ MPa m}^{0.5}$  has some merit for a defined set of steels when no other information is available. It is quite close to the “common-sense” value for bainite in Fig. 6 but it would be extremely conservative for the martensitic condition. It would be unsafe for the 300M steel tested at 77K (Fig. 4). Any physically-based lower bound might be expected to increase with test temperature, following perhaps the RKR prediction, which suggests a weak increase, because the yield strength, and hence the maximum stress generated in the process zone ahead of the crack-tip, decreases with increase in temperature.

## 6 FINAL REMARKS

Whether or not extrapolation to low failure probabilities is viable or not requires a clear distinction between what is “quasi-homogeneous” and what is “heterogeneous”. Judgement is involved. The following procedure is proposed:

- i) Plot fracture toughness results as a CDF on *normal* probability paper;
- ii) *If* the line is straight *and* the s.d. equates to that for random experimental errors (or a “pragmatic” value of  $<6 \text{ MPa m}^{0.5}$ ) class the material as “quasi-homogeneous” and extrapolate with some confidence (noting the need to identify, and investigate the causes of, outliers). Note that any exceptionally low, or negative, “lower bound” value is indicative of spatially heterogeneous material. There are strong suggestions of this, not only in the microstructures deliberately produced to generate Fig. 6, but also in the French A508 tensile results in Fig. 1, in the Beremin  $\sigma_F$  results, and in the Euro data-base.
- iii) If ii) is not satisfied, class the material as “heterogeneous”. “Forensic fractography” must then be employed to determine the more brittle constituent. If the ability of the tougher phase to arrest cracks formed in the more brittle phase were understood to the extent that it could be quantified, it might prove possible to use a weighted distribution directly to estimate the lower-bound, but, at present, the safest approach is to model the more brittle phase microstructurally and to carry-out fracture toughness tests on this (quasi-homogeneous) microstructure. These data can then be used for extrapolation purposes to determine the lower bound. In many cases, it will not be possible to have access to materials or to have sufficient time and resource to perform the necessary fractography and testing to follow such a detailed sequence. It is, however, important to appreciate the general effects of spatial heterogeneity, because the understanding gained leads to more intelligent “expert judgment”, to more confidence in the “data-mining” of other existing data-bases and to more precision in identifying what is “like-with-like”. Particularly to treat low-probability events, it is critically important to underpin analysis of fracture results with good metallurgical knowledge and appropriate micro-mechanical models.

## ACKNOWLEDGEMENTS

The results analysed have appeared (in other forms) in referenced open literature, but thanks are due to Prof.P.Bowen, Dr.J.E.King, Dr.D.J.Neville, Dr.M.Novovic, Dr.S.Slatcher, Dr.B.Wiltshire, Dr.S.Wu and Dr.X.Zhang for access to their original experimental results.

## REFERENCES

- ASTM Standard Test Method for Determination of Reference Temperature,  $T_0$ , for Ferritic Steels in the Transition Range E1921-02 (2002).
- Beremin *Metall. Trans.* **14A**, 2277-2287 (1983).
- Bompas-Smith, J.H. (*Mechanical Survival: the use of reliability data* (McGraw-Hill) (1973).
- Curry, D.A. and Knott, J.F. *Metal Science*, **13**, 341-346. (1979).
- Griffiths, J.R. and Owen D.R.J. *J Mech Phys Solids* **19**, 419-431 (1971).
- Islam, A., Bowen, P. and Knott, J.F. *Grain Boundaries: Their Characterisation and Influence on Properties*, edited by I.R.Harris and I.P.Jones (IOM Communications Ltd.), 55-72 (2001).
- King, J.E. and Knott, J.F. (1980) *J. Mech. Phys. Solids*, **28**, 191-201. (1980).
- Knott, J.F. (1994) *Advances in Fracture Resistance and Structural Integrity*, edited by V.V.Panasyuk *et al.* (Pergamon), 13-50 (1994).
- Knott, J.F. *Fracture, Plastic Flow and Structural Integrity*, edited by Peter Hirsch and David Lidbury IOM Communications Ltd.), 21-43 (2000).
- Lin, T., Evans, A. G., Ritchie, R. O. *J. Mech. Phys. Solids* **34**, 477-497.(1986).
- Lin, T., Evans, A. G., Ritchie, R. O. *Acta Metall.* **34**, 2205-2216. (1986).
- Marshall, W. *An Assessment of the Integrity of PWR Pressure Vessels* (Study Group Second Report) UKAEA, Fig. 3.7 and refs. (1982).
- May, M.J. (1965) *Review of Developments in Plane Strain Fracture Toughness Testing*, edited by W.F. Brown Jr. (ASTM STP 463) 42-62. (1965)
- Neville, D.J. and Knott, J.F. (1986) *J. Mech. Phys. Solids*, **34**, 243-291 (1986).
- Newmann A., Benois F.F. and Hibbert, K. *Schweisstechnik* (Berlin)**18**, 385-397 (1968).
- Ritchie, R.O., Knott, J.F., and Rice, J.R. *J. Mech. Phys. Solids*, **21**, 395-410 (1973).
- Slatcher, S. and Knott, J.F. *Fracture and the Role of Microstructure* (Proc. 4<sup>th</sup> Europ. Conf.on Fracture), edited by K.L Maurer and F.E.Matzer (EMAS Publishing), 174-181 (1982).
- Smith, E., Cook, T.S. and Rau, C.A. *Fracture 1977* (Proc. 4th Intl. Conf. on Fracture), edited by D.M.R.Taplin (University of Waterloo Press; also Pergamon 1978), 215-236. (1977).
- Sokolnikov, I.S. and Redheffer, R.M. *Mathematics of Physics and Modern Engineering* – second edition (McGraw-Hill Book Company) 642-645. (1966).
- Todinov, M.T., Novovic, M., Bowen, P., and Knott, J.F. *Mater. Sci. and Eng.* **A287**, 116-124 (2000)
- Tweed, J.H. and Knott, J.F. *Acta. Metall.* **35**, 1401-1414 (1987).
- Wallin, K. (2002) *Eng. Fract.. Mech* **69**, 451-481 (2002).
- Widgery, D.J. and Knott, J.F. *Metal Science*, **12**, 8-16.(1978).
- Wiltshire, B. and Knott J.F. *Intl. Jnl. of Fracture*, **16**, R19-R26 (1980).
- Wu, S. and Knott J.F. *J. Mech. Phys. Solids* **52**, 907-924 (2004).
- Zhang, X. and Knott, J.F. *Acta Mater.* **47**, 3483-3495 (1999).
- Zhang, X. and Knott, J.F. *Acta Mater.* **48**, 2135-2146 (2000).

